Extension of the zinc paratacamite phase diagram: Probing the effect of spin vacancies in an S = 1/2 kagome antiferromagnet

Extension of the zinc paratacamite phase diagram: Probing the effect of spin vacancies in an $S = \frac{1}{2}$ kagome antiferromagnet

M. A. de Vries,[1,*] D. Wulferding,[2] P. Lemmens,[2] J. S. Lord,[3] A. Harrison,[1,4] P. Bonville,[5] F. Bert,[6] and P. Mendels[6]

[1]*CSEC and School of Chemistry, The University of Edinburgh, Edinburgh EH9 3JZ, United Kingdom*

[2]*Institute for Condensed Matter Physics, TU Braunschweig, Mendelssohnsstrasse 3, D-38106 Braunschweig, Germany*

[3]*ISIS Facility, Rutherford Appleton Laboratory, Chilton, Didcot, Oxon OX11 OQX, United Kingdom*

[4]*Institut Laue-Langevin, 6 rue Jules Horowitz, F-38000 Grenoble, France*

[5]*Service de Physique de l'État Condensé, DSM, CEA Saclay, F-91191 Gif-sur-Yvette Cedex, France*

[6]*Laboratoire de Physique des Solides, Universite Paris X, Orsay, France*

(Received 9 November 2011; revised manuscript received 8 January 2012; published 20 January 2012)

We report on the extension of the phase diagram of the magnetic model system zinc paratacamite, $Zn_xCu_{4-x}(OH)_6Cl_2$ ($0 \leqslant x \leqslant 1$), with compositions $x > 1$, up to ∼1.2. This amounts to diamagnetic doping of the kagome lattice of antiferromagnetically coupled Cu^{2+} with $S = 1/2$ in what was hitherto known as the end member in the series: herbertsmithite of stoichiometry $ZnCu_3(OH)_6Cl_2$. Combining chemical analysis, x-ray diffraction, magnetic susceptibility measurements, Raman spectroscopy and muon spin relaxation spectroscopy we conclude the following: (i) Herbertsmithite can be synthesized in stoichiometric form, but it is affected by antisite disorder of ∼7% in Cu^{2+} content, implying that for $x = 1$, ∼7% of the Cu kagome sites is occupied by Zn^{2+}. (ii) The Zn content can be increased up to $x \sim 1.2$. No qualitatively new behavior is found for the diamagnetically doped kagome lattice, only a continuation of the trends observed for samples with $x < 1$ as x is increased.

DOI: 10.1103/PhysRevB.85.014422 PACS number(s): 75.30.−m, 75.40.Cx, 78.30.Am, 76.75.+i

I. INTRODUCTION

The mineral herbertsmithite, the $x = 1$ member of the zinc paratacamite family $Zn_xCu_{4-x}(OH)_6Cl_2$ with $0 \leqslant x \leqslant 1$, has attracted widespread attention as a Mott insulator in which the localized, antiferromagnetically coupled $S = 1/2$ spins are geometrically frustrated.[1–4] When antiferromagnetically coupled spins are arranged in three-dimensional (3D) lattices based on tetrahedra or 2D lattices based on triangles, then these spins cannot align antiferromagnetically with all neighboring spins. They are subject to competing constraints arising from the geometry of the lattice [see Fig. 1(a)]. Such antiferromagnets are called geometrically frustrated.[5] For some lattices, most notably the kagome lattice [Fig. 1(b)] of corner sharing triangles, this frustration is thought to completely suppress the "crystallization" of the spins into an ordered antiferromagnetic (Néel -type) ground state. The precise nature of the novel ground state that is expected to occur in ideal cases has been the subject of much theoretical work. In herbertsmithite and a small number of layered and 3D materials, including the vanadium (IV) oxyfluoride $[NH_4]_2[C_7H_14N][V_7O_6F_{18}]$,[6] $EtMe_3Sb[Pd(dmit)_2]_2$,[7] and $Na_4Ir_3O_8$,[8] no freezing of the local moments is observed at the lowest accessible temperatures despite strong antiferromagnetic exchange interactions. These materials provide exciting opportunities for the first experimental studies of spin liquid states. These Mott-insulating states not "dressed" by antiferromagnetic long-range order can lead to a better understanding of antiferromagnetic insulators in general.[3]

For $S = 1/2$, the huge ground-state degeneracy of the classical kagome antiferromagnet[9–11] is thought to be lifted[12,13] in favor of a macroscopically coherent quantum state.[14,15] This state is best seen as a hybrid of all possible arrangements of spin singlet (valence bond) dimerizations between spins, in analogy to the resonating valence bond (RVB) states in organic molecules such as benzene.[16] According to recent work using dynamic renormalization-group calculations, the RVB state is characterized by an energy gap from the nonmagnetic ground state to the first magnetic excited states.[17] Other work suggests that the suppression of any spontaneous symmetry breaking due to quantum fluctuations leaves a quantum-critical phase—a stable phase with the spatial and temporal correlations generally observed in critical phase transitions.[18–20] This so-called algebraic spin liquid, referring to the type of scaling of the spin-spin correlations with temperature in the critical state, is gapless and the ground state can have a nonzero magnetic susceptibility.

There is now strong evidence that the magnetic ground state of herbertsmithite is a gapless spin liquid, i.e., displaying a continuum of magnetic excitations; no freezing of spins is observed down to 50 mK, not even into a glassy state, as is conclusively demonstrated using μSR,[21] while the energy scale of the antiferromagnetic exchange is ∼200 K.[22,23] The magnetic susceptibility of the Cu ions on the kagome lattice approaches a nonzero value as $T \to 0$.[24–26] Furthermore, neutron spectroscopy data, measured at temperatures down to 50 mK and energies down to 0.1 meV, point to a continuum of magnetic excitations.[23,27,28] Hence, the spins do not disappear as $T \to 0$ nor do they freeze into a static arrangement. Neutron spectroscopy measurements show that the dynamic spin-spin correlations are near neighbor only, extend over a very wide range in energy (up to at least 23 meV), and depend only weakly on temperature up to 120 K.[27] It is precisely the temperature-independent, short-ranged dynamic correlations that have been put forward as a hallmark property of a quantum spin liquid.[29]

An appealing explanation of at least some of these observations is that the magnetic ground state is either in a

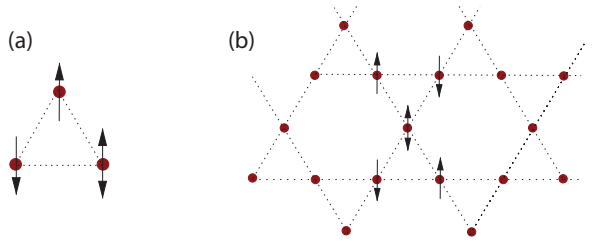

FIG. 1. (Color online) The principle of geometric frustration. There is no uniquely defined low-energy configuration for the antiferromagnetically coupled spins on a triangle (a) and on the kagome lattice (b).

quantum-critical phase, as predicted by Ran and Hermele and co-workers,[19,20] or at a quantum-critical point, for example due to a Dzyaloshinky-Moriya interaction.[30] However, in such a quantum critical state, the spin-spin correlation length diverges algebraically as the temperature is lowered, contrary to what is observed in herbertsmithite. One explanation for this discrepancy is the presence of quenched disorder in the kagome antiferromagnet. It has been suggested that spin vacancies on the kagome lattice in herbertsmithite result in a partially frozen, disordered arrangement of valence bonds—a state termed "valence bond glass"(VBG).[31]

The presence of structural disorder, in particular in the form of antisite disorder between the Cu^{2+} and the Zn^{2+} ions, has been a matter of debate.[32] A number of experimental probes point to the occupation of between 14% and 23% of the interplane Zn sites by Cu^{2+} ions, depending on the synthesis method and experimental probe.[24–26,33,34] The resulting "antisite" spins arising from Cu^{2+} ions located on the interplane Zn sites couple only weakly to the spins on the kagome layers (see Fig. 2). These defects are therefore easily detected as weakly coupled spins that can be treated using a mean-field Curie-Weiss picture, following a Brillouin function in the temperature/high-field magnetic susceptibility[24] and in the low-temperature heat capacity as a Schottky anomaly.[26] Clear signatures of the antisite spins have furthermore been identified in the ^{17}O NMR (Ref. 25) and ^{2}D NMR spectra.[34] For stoichiometric herbertsmithite (with Zn:Cu = 1:3, i.e., $x = 1$), the presence of antisite spins means an equal number of spin vacancies, or diamagnetically doped sites on the kagome lattice. These diamagnetically doped kagome sites do not have such clearly identifiable signatures in the bulk properties but have been observed using ^{17}O NMR.[25] Freedman *et al.*[33] have recently questioned the presence of Zn^{2+} ions on the kagome lattice, suggesting that what is held for the end member of the zinc paratacamite series, the zinc composition x is closer to 0.85 than to 1. This claim is based on new neutron diffraction and anomalous x-ray diffraction measurements[33,35] on single crystals. However, these crystals and the precursor powder sample were synthesized using a different method[33] from the one used for most studies on herbertsmithite reported in the literature up to 2010.[1] While this limits comparisons of results reported in Ref. 33 with previous work on herbertsmithite, it is possible that the antisite disorder in their sample is reduced. However, it can be concluded that the herbertsmithite samples synthesized following Shores *et al*[1] are stoichiometric. Compositional analysis using inductively coupled plasma Auger electron spectroscopy (ICP-AES) has consistently indicated $x = 1.00$ for the end member in the series, even for single crystals.[36] In the course of our studies on herbertsmithite and other compounds of the zinc paratacamite family, a large number of ICP-EAS measurements have been carried out. We will discuss these measurements in detail in Sec. III, and we will show that the accuracy of this method is good enough to confirm the stoichiometry of herbertsmithite to within 1%. This implies that some Zn^{2+} ions occupy the Cu sites on the kagome lattice, approximately 7% for herbertsmithite synthesized following 1.

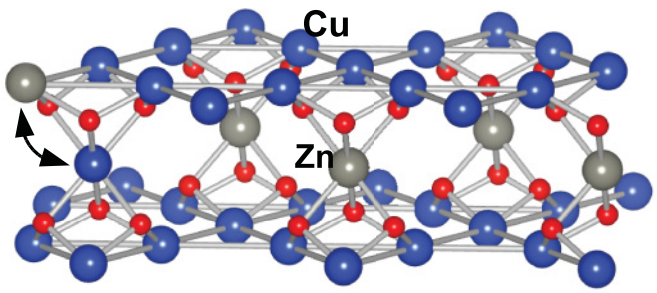

FIG. 2. (Color online) Two kagome layers with the Cu^{2+} ions (blue), the interlayer Zn^{2+} ions (gray), and the O^{2-} ions (red). The occupation that is illustrated is for $x = 1$ (also known as herbertsmithite). Due to antisite disorder at $x = 1.0$, roughly one of every five Zn sites contains a Cu^{2+} ion, with a Zn^{2+} ion occupying a Cu site at the kagome lattice.

To confirm the presence of diamagnetic Zn^{2+} ions on the kagome lattice for herbertsmithite [$Zn_xCu_{4-x}(OH)_6Cl_2$, $x = 1$] and to understand how they affect the cooperative properties of the $S = 1/2$ kagome antiferromagnet, we synthesized samples with $1 < x < 1.2$ using a modified synthesis. These samples are compared with other compositions, $x = 0.85, 0.9$, and 1.0. Muon spin relaxation spectra (Sec. VII), magnetic susceptibility, and Raman spectra (Sec. VI) are presented, and the observed dependence on x of the cooperative properties is compared with theory. It has been predicted that a small number of diamagnetic impurities leads to a reduced susceptibility at low temperatures due to the formation of static spin singlets around the vacancies,[37,38] shifting the spectral weight of magnetic excitations to higher energies.

II. CHEMICAL SYNTHESIS

Zinc paratacamite with $0 \leqslant x \leqslant 1$ is synthesized hydrothermally[1] from a mixture of $Cu_2(OH)_2CO_3$, $ZnCl_2$ and $CuCl_2$, where the ratio between the latter two ingredients determines the zinc content x following Table I. We found that compounds with $x > 1$ with increased Zn^{2+} occupancy of the kagome Cu sites can be synthesized by substituting some of the $Cu_2(OH)_2CO_3$ with $2ZnCO_3{\cdot}3Zn(OH)_2 \cdot nH_2O$, as indicated in Table I.

The synthesis was carried out in a 23 mL acid digestion bomb, heated to 210 °C for 24 h in a box furnace, and cooled down slowly, at a rate of 0.1 °C/min. The precipitate was filtered and dried in air, yielding 0.75 g of product. The stoichiometries given in Table I were obtained using inductively coupled plasma Auger electron spectroscopy (ICP-AES), with an experimental error of ∼3% in Zn content. The

TABLE I. The used mass in grams of all ingredients to be added to 10 mL of water in a 23 mL bomb liner, to obtain zinc paratacamite with Zn content x. The values for $x \leqslant 1$ are from Shores *et al.*[1] The values for $x > 1$ (diamagnetically doped kagome) are as found in this study, using $2ZnCO_3{\cdot}3Zn(OH)_2 \cdot nH_2O$ (in the table noted as $ZnCO_3$ . . .).

$ZnCl_2$	$CuCl_2 \cdot 2H_2O$	$Cu_2(OH)_2CO_3$	$ZnCO_3$ . . .	$x(\pm 0.02)$
0.0	0.426	0.662	0.0	0.0
0.136	0.257	0.662	0.0	0.30
0.271	0.085	0.662	0.0	0.66
0.300	0.024	0.662	0.0	0.9
0.310	0.0	0.662	0.0	1.0
0.310	0.0	0.640	0.024	1.10
0.310	0.0	0.574	0.096	1.40

masses used in Table I were interpolated and extrapolated up to $x \sim 1.7$, but for $x > 1.2$, impurity phases were present in the x-ray diffraction (XRD) patterns. Hence our analysis will focus on samples with $x < 1.2$.

III. ELEMENTAL ANALYSIS

ICP-AES is the most reliable tool in determining the stoichiometry of samples and plays a crucial role in this work. Following the doubts raised about the accuracy of the method,[33] ICP-AES data from our 22 herbertsmithite samples were reanalyzed. The mean zinc content $x[=4/(N_{Cu}/N_{Zn}+1)]$ of these measurements is 0.991, and the standard deviation is 0.03, as reflected in the stated error bar for a single measurement. With 22 measurements, the error in the mean of $x = 0.991$ is 0.007. Similar numbers are obtained for repeated measurements of the same sample; one herbertsmithite sample was measured $N = 5$ times, with mean $x = 1.014$ and standard deviation $\sigma = 0.025$, giving an error in the mean of $\sigma/\sqrt{N} = 0.01$. This is only our own data. We could add to this the data published in other papers, including Refs. 1, 39, and 33. The nominal off-stoichiometry of herbertsmithite is then confirmed to be well below 1% in zinc content. This means that it can be ruled out that for herbertsmithite, $x = 0.85$, as claimed in Ref. 33. The heat capacity and magnetic susceptibility from the samples used by Han[36] and Freedman *et al.*[33] suggest the degree of antisite disorder might be 1–2% lower than for samples grown using the most established synthesis method.[1]

IV. X-RAY DIFFRACTION

The sample with the diamagnetically doped kagome lattice for which all experiments described here were carried out had $x = 1.16 \pm 0.02$. The diffraction pattern for this sample is shown in Fig. 3. The pattern was Rietveld-analyzed using the General Structure Analysis Program,[40] with residuals $\chi^2 = 5.1$, $R_{wp} = 6.15\%$, and $R_p = 4.63\%$. We found lattice parameters $a = 6.816\,74(4)$ Å and $c = 14.0208(2)$ Å compared to the reported values of $a = 6.8342(3)$ Å and $c = 14.0320(12)$ Å.[1]

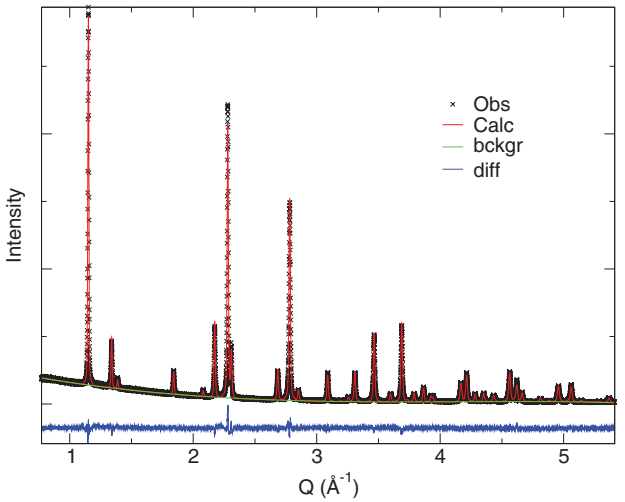

FIG. 3. (Color online) The x-ray diffraction pattern (black ×) for $x = 1.16$ zinc paratacamite, with structure refinement (red) and the difference (blue).

The refinement is of comparable quality to the refinements of diffraction data of $x = 1$ samples (with typically $\chi^2 = 2.2$, $R_{wp} = 7.3\%$, and $R_p = 5.4\%$).[26]

V. MAGNETIC SUSCEPTIBILITY

The magnetic susceptibility was measured on a number of ~80 mg samples with compositions x in the range $0.85 < x < 1.2$ using a Quantum Design MPMS Squid magnetometer and in a vibrating sample magnetometer (VSM).

As mentioned earlier, the Curie tail, which dominates the low-temperature susceptibility, arises from the antisite spins because these spins are weakly coupled to the spins on the kagome layers. Including this Curie contribution, the induced magnetization per formula unit is given by

$$M(H) = fg\mu_B S B_S\left(\frac{gS\mu_B H}{k_B T^*}\right) + c\chi_k H, \qquad (1)$$

where B_S is the Brillouin function, $T^* = T - T_{CW} = 1.7 - T_{CW}$, f is the fraction of Cu^{2+} spins on the Zn sites, and c is the fraction of spins on the kagome sites with susceptibility χ_k. The spin quantum number $S = 1/2$ and we used $g = 2.2$. Following Bert *et al.*,[24] this Curie-like contribution was measured in a VSM in fields up to 14 T and at 1.7 K to fully saturate the magnetization from these nearly free spins. As is clear from Fig. 4, the magnetization versus field dependence of $x = 0.85$, 0.9, and 1.16 is very similar to that reported earlier for $x = 1$.[24] Above approximately 8 T, the weakly coupled spins (f per unit cell) are fully aligned with the field so that the gradient dM/dH observed for $H > 8$ T directly yields the susceptibility of the kagome layers χ_k, listed in the last column of Table II. Note that the values of χ_k shown here are per mol Cu^{2+} ions that are actually located in the kagome planes, calculated using $c = 4 - x - f$ in column 4 of Table II. This explains the difference from the value reported in Ref. 24, 1.5×10^{-3} emu/mol Cu, including *all* copper ions. As shown in Table II, the number of diamagnetic defects on the kagome lattice goes from $7.5 \pm 1\%$ for $x = 1$ to $11.8 \pm 1\%$ for $x = 1.16$. This is a significant increase that,

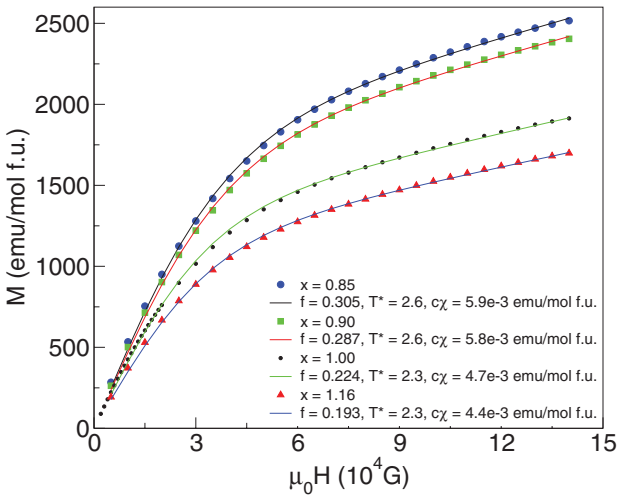

FIG. 4. (Color online) The magnetization as a function of field for $x = 0.85$ (blue dots), $x = 0.9$ (green squares), $x = 1$ (black bullets, from Ref. 24), and $x = 1.16$ (red triangles). The lines through the data are fits with Eq. (1).

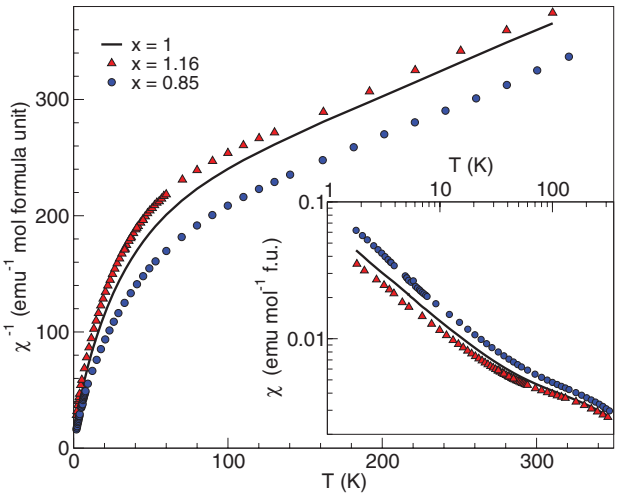

FIG. 5. (Color online) The inverse magnetic susceptibility of $x = 1.0$ (black line), 1.16 (red triangles), and 0.85 (blue dots) samples measured in 100 G. The inset shows the magnetic susceptibility on a log-log scale.

it will be shown, has clearly observable consequences for the cooperative properties of the system.

Figure 5 shows the temperature dependence of the inverse magnetic susceptibility for samples with $x = 0.85$, 1.00, and 1.16, measured in 100 G. The $x = 1.1$ data are very close to the $x = 1$ data and are not shown. The main panel shows the inverse susceptibility revealing a linear Curie-Weiss regime above ∼120 K for all x. The effective moments as obtained from Curie-Weiss fits are for all samples around 0.58 emu/mol Cu, large compared to the expected Curie constant of 0.37 emu/mol Cu^{2+} but consistent with other published data.[1,23,24] The Weiss temperatures as obtained from the Curie-Weiss fits for $x = 0.85$, 1.0, and 1.16 are −280(20), −300(20), and −340(30) K, respectively. This trend is a continuation of the approximately linear trend as a function of x as observed previously.[1] The reduction of the Weiss temperature (toward more negative values) as x is increased suggests that removing Cu^{2+} spins on the interplane (Zn) sites equates to a removal of ferromagnetic exchange interactions, consistent with the small ferromagnetic moment that develops below 6 K for $0 \leqslant x \leqslant 0.5$. The removal of these ferromagnetic bonds between the spins on the interplane Zn sites and in the kagome layers continues for $x > 1$, but at the same time strongly antiferromagnetically coupled spins on the kagome lattice are removed, leading to a reduction of antiferromagnetic bonds. This could be expected to make the system easier to magnetize in a field and raise the Weiss temperature in the direction of positive (ferromagnetic) values, contrary to what is actually observed. This (apparent) increase of antiferromagnetic correlations, further suppressing the high-temperature susceptibility, could be taken as a sign of the predicted formation of stable spin singlets around diamagnetic defects in the kagome lattice.[37,38] This is also consistent with the reduction of χ_k at 1.7 K as obtained from Fig. 4. The inset of Fig. 5 shows the magnetic susceptibility against temperature on a log-log scale, revealing again the low temperature Curie tail.

TABLE II. The Cu occupancies on the kagome lattice as a function of zinc content x, obtained by combining ICP-AES data and fits of Eq. (1) to the data in Fig. 4. The second column gives the number of nearly free spins detected per unit cell f. The third column is the Weiss temperature. $c = 4 - x - f$ is the number of Cu ions per unit cell occupying the three kagome sites. The fourth column is the Cu occupancy of the kagome sites as a percentage. The last column gives the susceptibility per Cu^{2+} ion on the kagome layers χ_k in emu/mol Cu_k. The error in c is about 1% and the error in χ_k is ∼4%.

$x \pm 0.03$	$f \pm 0.01$	T_{CW} (K)	c	$c/3 \times 100\%$	χ_k emu/mol Cu
0.85	0.305	−0.9	2.84	95.0	2.08×10^{-3}
0.90	0.287	−0.9	2.81	93.8	2.06×10^{-3}
1.00	0.224	−0.6	2.78	92.5	1.69×10^{-3}
1.16	0.193	−0.6	2.65	88.2	1.66×10^{-3}

VI. RAMAN SPECTROSCOPY

Raman scattering measurements were performed in quasi-backscattering geometry, using a frequency-doubled Nd:YAG laser ($\lambda = 532.1$ nm) with 15 mW laser power and a focus diameter of about 100 μm. The scattered light was analyzed via a triple spectrometer by a liquid-nitrogen-cooled CCD. The acquisition time was 10 s, and 60 accumulations were taken to increase the signal-to-noise ratio. All measurements were performed under ambient conditions and at room temperature.

Figure 6(a) shows the Raman spectra for samples of different stoichiometry ($0.5 \leqslant x < 1.2$). We observe seven major Raman modes that correspond to the Cl and O sites of the space group $R\bar{3}m$ with $\Gamma_{\text{Raman}} = 3A_{1g} + 4E_g$. All of these modes are observed in our spectra. Additionally, for all samples apart from $x = 0.5$, an asymmetric Fano-like feature at 230 cm^{-1} is observed. Such a feature can in general be induced by structural disorder or coupling to a continuum of magnetic degrees of freedom. A continuum of magnetic fluctuations has actually been observed in neutron spectroscopy data, extending

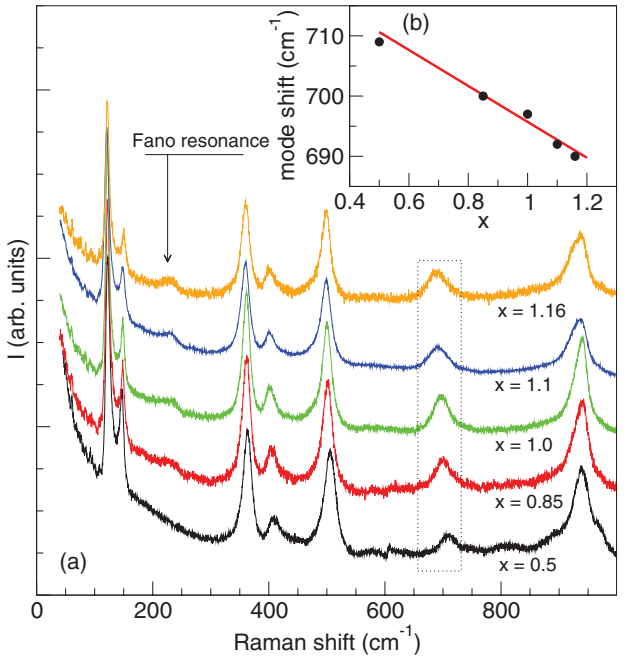

FIG. 6. (Color online) (a) Raman spectra for $Zn_xCu_{4-x}(OH)_6Cl_2$ with $x = 0.5$, 0.85, 1.0, 1.1, and 1.16. The spectra are shifted in intensity for clarity. (b) The linear frequency dependence of the phonon mode at 700 cm^{-1} [indicated by the box in panel (a)], with the Cu/Zn ratio.

up to at least 25 meV and 120 K.[27] The Fano resonance is therefore ascribed to the coupling of a phonon mode to this continuum of magnetic excitations. It should be noted that this continuum of antiferromagnetic fluctuations persists down to the lowest accessible temperatures, which is consistent with the temperature dependence of the Fano resonance.[41] Remarkably, the intensity of this mode is decreasing with decreasing x until it is no longer observable for $x = 0.5$. The diminishing intensity of the Fano resonance of the room-temperature spin dynamics could be related to the change in the magnetic ground state as the 3D connectivity of the lattice is increased with lower x, from spin liquid to cluster glass, as observed using μSR.[21]

With increasing substitution of Cu^{2+} for Zn^{2+}, the phonon mode at around 700 cm^{-1} clearly shifts to lower energy while modes at lower frequencies do not change. This trend is illustrated in Fig. 6(b). For all compositions, this shift can be described by a linear dependence on composition x following

$$E_{\text{phonon}}\ (\text{cm}^{-1}) = 725.7 - 30.2x. \qquad (2)$$

The observed shift that continues for $x > 1$ is a qualitative confirmation that substitution of Cu with Zn on the kagome lattice has been achieved.

VII. MUON SPIN RELAXATION SPECTROSCOPY

Muon spin rotation/relaxation (μSR) spectra were measured on samples with $x = 0.85$ and 1.16, and compared with data on $x = 1.0$ as published in Ref. 21. The measurements were carried out at the MUSR station at ISIS. A dilution refrigerator was used for measurements between 100 mK and 1.5 K. Positive muons were stopped in pellet-pressed samples of zinc paratacamite of 1–2 mm thickness. The zero-field muon relaxation at high temperatures has shown that there are two different muon stopping sites; 80–90% of the muons bond with the OH^- group in the superexchange pathway between neighboring Cu^{2+} ions, forming an OH-μ complex.[42] The remaining muons stop close to the Cl^- site, showing a Gaussian Kubo-Toyabe relaxation. The asymmetry (A) in the forwards/backwards emitted positrons arising from the muon decay were corrected for a constant background (BG), which is due to muons stopping outside of the sample. The time dependence of the muon polarization given by $P(t) = [A(t) - \text{BG}]/[A(t = 0) - \text{BG}]$ is analyzed here.

The local magnetic fields due to the nuclear moments are less than 10 G. Hence, a magnetic field of 80 G applied along the initial muon polarization (longitudinal) was applied to decouple the muon relaxation from the static nuclear moments and probe the much stronger fields from the unpaired electron spins in the sample. The resulting relaxation spectra for $x = 1.0$, 0.85 and 1.16 are shown in Figs. 7(a), 7(b), and 7(c), respectively.

In the paramagnetic phase, the muon relaxation due to electronic moments is very small because the moments fluctuate too fast to be probed by the muons. As first reported for herbertsmithite ($x = 1$) in Ref. 21 and also shown in Fig. 7(a), no static electronic moments are detected even at the lowest temperatures accessed, down to 40 mK. There is, however, a qualitative change in the muon relaxation around 1.5 K. Below this temperature, there is a clear increase in

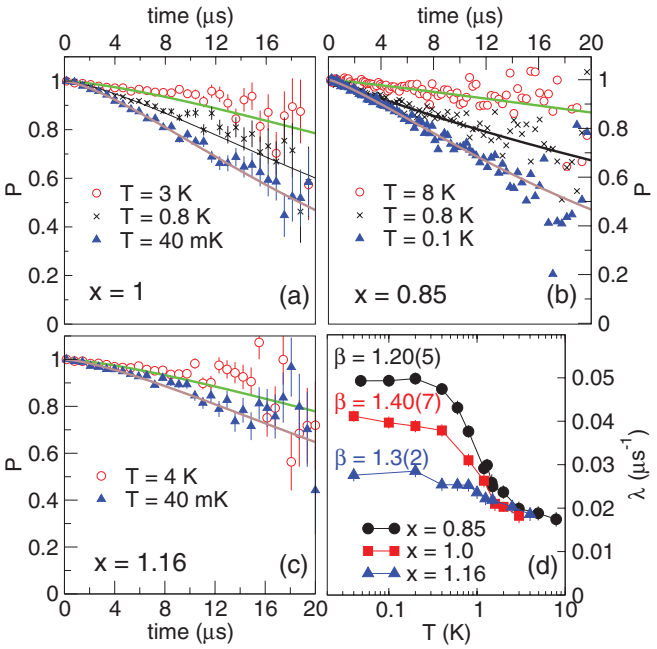

FIG. 7. (Color online) (a) The muon polarization for $x = 1.0$ in a longitudinal field of 80 G at 3 K (red dots), 0.8 K (black crosses), and 40 mK (blue triangles). (b) The muon polarization for $x = 0.85$ at 8 K (red dots), 0.8 K (black crosses), and 0.1 K (blue triangles). (c) The muon polarization for $x = 1.16$ at 4 K (red dots) and 40 mK (blue triangles). (d) The relaxation rates λ for $x = 0.85$ (black), $x = 1.0$ (red), and $x = 1.16$ (blue) as a function of temperature. The low-temperature compression exponents β for each composition are indicated in the corresponding color.

the relaxation rate and the muon relaxation smoothly changes from exponential decay to compressed exponential.

For samples with x between 0.66 and 1.16, the muon relaxation in a longitudinal field of 80 G can be fitted by a modified exponential decay

$$P(t) = \exp\left[-(\lambda t)^{\beta}\right], \tag{3}$$

where λ is the relaxation constant. Above 1.5 K, $\beta = 1$ for all samples. For $x = 0.6, \ldots, 1$, β increases gradually below 1.5 K (Ref. 21) along with the relaxation rates as shown in Fig. 7(d). The base temperature relaxation rate increases as x is lowered due to the increased connectivity of the lattice, while β increases as x is increased up to $x = 1$. Because the relaxation rate for $x = 1.16$ is so small, β cannot be determined with the same accuracy as for $x = 1$, but it does remain >1. A similar trend in relaxation rate as a function of the composition was observed in a study involving the Mg analog of zinc paratacamite, $Mg_xCu_{4-x}(OH)_6Cl_2$.[43]

The $\beta > 1$ in Eq. (3) acts to compress the muon decay some way toward a Gaussian relaxation. A smooth development of β from 1 to 2 has previously been observed in SCGO[44] and BSZCGO[45] at the spin-glass transition to a glassy state with relatively slow dynamics. As in herbertsmithite, the muon relaxation in SCGO and BSZCGO cannot be decoupled by a field, indicating that the muon relaxation is due to spin fluctuations in the ground state. The situation in zinc paratacamite with $x \sim 1$ is, however, still quite different; even in the paramagnetic phase with T just above T_g in SCGO, the muon relaxation is faster than for stoichiometric herbertsmithite at 40 mK. Furthermore, both λ and β saturate below $\sim$200 mK, with β significantly less than 2. Hence, the increase in β as a function of temperature for $x \sim 1$ cannot be understood as a crossover to a spin-glass state, which would give $\beta = 2$ and full muon relaxation well within the 10 μs time window. Rather, the compression exponent 1.4 in the muon relaxation is characteristic of the ground state for $x \sim 1$, and likely a reflection of the anomalous spin dynamics observed in neutron spectroscopy data.[27,28]

VIII. CONCLUSION

The presented results confirm that stoichiometric herbertsmithite can be synthesized but that it is affected by Cu/Zn antisite disorder involving $\sim$7% of the Cu^{2+} ions. To understand the effect of diamagnetic Zn^{2+} ions replacing Cu^{2+} on the kagome sites, leading to a diamagnetic doping of the magnetic lattice, the zinc paratacamite family has been extended with phases $1 < x < 1.2$. The successful substitution of Cu^{2+} with Zn^{2+} on the kagome sites is quantified using elemental analysis and magnetic susceptibility measurements at 1.7 K in fields up to 14 T. It is shown that for $x = 1.16$, approximately 11% of the Cu kagome sites are occupied by Zn^{2+}. The magnetic susceptibility up to room temperature, the Raman spectra, and the muon spin relaxation spectra are compared with samples with a lower Zn content, with $x = 0.85, 0.9$ and stoichiometric herbertsmithite ($x = 1$). The trend of increasingly fast spin-dynamics in the ground state with increasing x continues for $x > 1$, at least up to $x \sim 1.2$.

ACKNOWLEDGMENTS

M.d.V. wishes to thank G. Nichol (University of Edinburgh) for his assistance with x-ray diffraction measurements. Part of the work was supported by the IGSM, Braunschweig.

*m.a.devries@ed.ac.uk

[1] M. P. Shores, E. A. Nytko, B. M. Bartlett, and D. G. Nocera, J. Am. Chem. Soc. **127**, 13462 (2005).
[2] F. Bert *et al.*, J. Phys.: Conf. Ser. **145**, 012004 (2009).
[3] P. A. Lee, Science **321**, 1306 (2008).
[4] P. Mendels and F. Bert, J. Phys. Soc. Japan **79**, 011001 (2010).
[5] A. P. Ramirez, Annu. Rev. Mater. Sci. **24**, 453 (1994).
[6] F. H. Aidoudi *et al.*, Nat. Chem. **3**, 801 (2011).
[7] M. Yamashita *et al.*, Science **328**, 1246 (2010).
[8] Y. Okamoto, M. Nohara, H. Aruga-Katori, and H. Takagi, Phys. Rev. Lett. **99**, 137207 (2007).
[9] J. N. Reimers, A. J. Berlinsky, and A.-C. Shi, Phys. Rev. B **43**, 865 (1991).
[10] J. T. Chalker, P. C. W. Holdsworth, and E. F. Shender, Phys. Rev. Lett. **68**, 855 (1992).
[11] I. Ritchey, P. Chandra, and P. Coleman, Phys. Rev. B **47**, 15342 (1993).
[12] P. Fazekas and P. W. Anderson, Philos. Mag. **30**, 423 (1974).
[13] G. Misguich and C. Lhuillier, in *Two-dimensional Quantum Antiferromagnets*, edited by H. T. Diep (World Scientific, Singapore, 2004), pp. 229–306.
[14] P. W. Anderson, Science **235**, 1196 (1987).
[15] L. Balents, Nature (London) **464**, 199 (2010).
[16] L. Pauling, *The Nature of the Chemical Bond*, 3rd ed. (Cornell University Press, Ithaca, NY, 1960).
[17] S. Yan, D. A. Huse, and S. R. White, Science **332**, 1173 (2011).
[18] M. Hermele, T. Senthil, and M. P. A. Fisher, Phys. Rev. B **72**, 104404 (2005).
[19] Y. Ran, M. Hermele, P. A. Lee, and X.-G. Wen, Phys. Rev. Lett. **98**, 117205 (2007).
[20] M. Hermele, Y. Ran, P. A. Lee, and X.-G. Wen, Phys. Rev. B **77**, 224413 (2008).
[21] P. Mendels, F. Bert, M. A. de Vries, A. Olariu, A. Harrison, F. Duc, J. C. Trombe, J. Lord, A. Amato, and C. Baines, Phys. Rev. Lett. **98**, 077204 (2007).
[22] G. Misguich and P. Sindzingre, Eur. Phys. J. B **59**, 305 (2007).
[23] J. S. Helton *et al.*, Phys. Rev. Lett. **98**, 107204 (2007).
[24] F. Bert, S. Nakamae, F. Ladieu, D. L'Hote, P. Bonville, F. Duc, J. C. Trombe, and P. Mendels, Phys. Rev. B **76**, 132411 (2007).
[25] A. Olariu, P. Mendels, F. Bert, F. Duc, J. C. Trombe, M. A. de Vries, and A. Harrison, Phys. Rev. Lett. **100**, 087202 (2008).
[26] M. A. de Vries, K. V. Kamenev, W. A. Kockelmann, J. Sanchez-Benitez, and A. Harrison, Phys. Rev. Lett. **100**, 157205 (2008).
[27] M. A. de Vries, J. R. Stewart, P. P. Deen, J. Piatek, G. N. Nilsen, H. M. Ronnow, and A. Harrison, Phys. Rev. Lett. **103**, 237201 (2009).

[28]J. S. Helton, K. Matan, M. P. Shores, E. A. Nytko, B. M. Bartlett, Y. Qiu, D. G. Nocera, and Y. S. Lee, Phys. Rev. Lett. **104**, 147201 (2010).
[29]G. Shirane, Y. Endoh, R. J. Birgeneau, M. A. Kastner, Y. Hidaka, M. Oda, M. Suzuki, and T. Murakami, Phys. Rev. Lett. **59**, 1613 (1987).
[30]O. Cepas, C. M. Fong, P. W. Leung, and C. Lhuillier, Phys. Rev. B **78**, 140405 (2008).
[31]R. R. P. Singh, Phys. Rev. Lett. **104**, 177203 (2010).
[32]P. Mendels and F. Bert, J. Phys.: Conf. Ser. **320**, 012004 (2011).
[33]D. E. Freedman *et al.*, J. Am. Chem. Soc. **132**, 16185 (2010).
[34]T. Imai, M. Fu, T. H. Han, and Y. S. Lee, Phys. Rev. B **84**, 020411 (2011).
[35]M. A. de Vries and A. Harrison, Nature (London) **468**, 908 (2010).
[36]T. H. Han, J. S. Helton, S. Chu, A. Prodi, D. K. Singh, C. Mazzoli, P. Muller, D. G. Nocera, and Y. S. Lee, Phys. Rev. B **83**, 100402 (2011).
[37]S. Dommange, M. Mambrini, B. Normand, and F. Mila, Phys. Rev. B **68**, 224416 (2003).
[38]K. Gregor and O. I. Motrunich, Phys. Rev. B **77**, 184423 (2008).
[39]S.-H. Lee *et al.*, Nat. Mater. **6**, 853 (2007).
[40]A. C. Larson and R. B. Von Dreele, Los Alamos National Laboratory Report LAUR 86-748 (2000) [http://www.ccp14.ac.uk/ccp/ccp14/ftp-mirror/gsas/public/gsas/manual/GSASManual.pdf].
[41]D. Wulferding, P. Lemmens, P. Scheib, J. Roder, P. Mendels, S. Chu, T. Han, and Y. S. Lee, Phys. Rev. B **82**, 144412 (2010).
[42]J. Lord, S. Cottrell, and W. Williams, Physica B **289-290**, 495 (2000).
[43]E. Kermarrec, P. Mendels, F. Bert, R. H. Colman, A. S. Wills, P. Strobel, P. Bonville, A. Hillier, and A. Amato, Phys. Rev. B **84**, 100401 (2011).
[44]Y. J. Uemura *et al.*, Phys. Rev. Lett. **73**, 3306 (1994).
[45]D. Bono, P. Mendels, G. Collin, N. Blanchard, F. Bert, A. Amato, C. Baines, and A. D. Hillier, Phys. Rev. Lett. **93**, 187201 (2004).